AJNR

3D Pseudocontinuous Arterial Spin-Labeling MR Imaging in the Preoperative Evaluation of Gliomas

Q. Zeng, B. Jiang, F. Shi, C. Ling, F. Dong and J. Zhang

AJNR Am J Neuroradiol 2017, 38 (10) 1876-1883
doi: https://doi.org/10.3174/ajnr.A5299
http://www.ajnr.org/content/38/10/1876

3D Pseudocontinuous Arterial Spin-Labeling MR Imaging in the Preoperative Evaluation of Gliomas

Q. Zeng, B. Jiang, F. Shi, C. Ling, F. Dong, and J. Zhang

ABSTRACT

BACKGROUND AND PURPOSE: Previous studies showed conflicting results concerning the value of CBF maps obtained from arterial spin-labeling MR imaging in grading gliomas. This study was performed to investigate the effectiveness of CBF maps derived from 3D pseudocontinuous arterial spin-labeling in preoperatively assessing the grade, cellular proliferation, and prognosis of gliomas.

MATERIALS AND METHODS: Fifty-eight patients with pathologically confirmed gliomas underwent preoperative 3D pseudocontinuous arterial spin-labeling. The receiver operating characteristic curves for parameters to distinguish high-grade gliomas from low-grade gliomas were generated. Pearson correlation analysis was used to assess the correlation among parameters. Survival analysis was conducted with Cox regression.

RESULTS: Both maximum CBF and maximum relative CBF were significantly higher in high-grade gliomas than in low-grade gliomas ($P < .001$). The areas under the curve for maximum CBF and maximum relative CBF in distinguishing high-grade gliomas from low-grade gliomas were 0.828 and 0.863, respectively. Both maximum CBF and maximum relative CBF had no correlation with the Ki-67 index in all subjects and had a moderate negative correlation with the Ki-67 index in glioblastomas ($r = -0.475, -0.534$, respectively). After adjustment for age, a higher maximum CBF ($P = .008$) and higher maximum relative CBF ($P = .005$) were associated with worse progression-free survival in gliomas, while a higher maximum relative CBF ($P = .033$) was associated with better overall survival in glioblastomas.

CONCLUSIONS: 3D pseudocontinuous arterial spin-labeling–derived CBF maps are effective in preoperative evaluation of gliomas. Although gliomas with a higher blood flow are more malignant, glioblastomas with a lower blood flow are likely to be more aggressive.

ABBREVIATIONS: ASL = arterial spin-labeling; CASL = continuous ASL; GBM = glioblastoma; HGG = high-grade glioma; HR = hazard ratio; KPS = Karnofsky Performance Scale; LGG = low-grade glioma; max = maximum; OS = overall survival; pCASL = pseudocontinuous ASL; PFS = progression-free survival; ROC = receiver operating characteristic; WHO = World Health Organization

Glioma is the most common intracranial malignant tumor, accounting for almost 80% of primary malignant brain tumors.[1] Grading of gliomas is important for an optimal therapy plan and predicting outcome.[2,3] According to the World Health Organization (WHO) criteria, gliomas can be classified into 4 groups: grades I–IV. Grade I and grade II gliomas are considered low-grade gliomas (LGGs), while grade III and grade IV gliomas are regarded as high-grade gliomas (HGGs).

Advanced MR imaging techniques, such as MR perfusion, have been shown to be more effective than conventional MR imaging techniques in grading gliomas.[4,5] Dynamic susceptibility contrast perfusion imaging is the reference standard for evaluating tumor perfusion.[6,7] However, this technique relies on the intravenous application of a contrast medium, which is not suitable for patients who are allergic to this medium or who have renal failure.[8,9]

Arterial spin-labeling (ASL) is a noninvasive MR perfusion imaging technique for obtaining CBF maps. Some previous studies based on pulsed ASL and continuous ASL (CASL) have shown that the ASL-derived CBF maps have potential value in grading gliomas[8,10-15] and predicting their progression.[9,16,17] However, although pseudocontinuous ASL (pCASL) is considered an improved method over pulsed ASL and CASL,[18-20] a recent study reported that pCASL-derived CBF maps failed to accurately grade gliomas.[21]

Received February 8, 2017; accepted after revision May 22.

From the Departments of Neurosurgery (Q.Z., C.L., J.Z.), Radiology (B.J., F.D.), and Neurology (F.S.), Second Affiliated Hospital of Zhejiang University School of Medicine, Hangzhou, Zhejiang, China; and Brain Research Institute (J.Z.) and Collaborative Innovation Center for Brain Science (J.Z.), Zhejiang University, Hangzhou, Zhejiang, China.

This work was supported by the Natural Science Foundation of Zhejiang (grant No. LY13H180006) and the Medicine and Health Research Foundation of Hangzhou (grant No. 20140633B25).

Please address correspondence to Jianmin Zhang, MD, Department of Neurosurgery, Second Affiliated Hospital of Zhejiang University School of Medicine, 88 Jiefang Rd, Hangzhou, Zhejiang, China, 310009; e-mail: zjm135@vip.sina.com

http://dx.doi.org/10.3174/ajnr.A5299

On the other hand, according to many previous studies, gliomas with higher tumor blood flow are commonly more malignant.[8-17] However, a recent study found a positive correlation between proliferation activity and levels of a hypoxia biomarker in glioblastoma (GBM),[22] suggesting that GBM with a lower blood flow might be more aggressive. Hence, the correlation between relative CBF and the grade of malignancy might be more complex in gliomas.

The purpose of this study was to examine the value of the CBF maps derived from 3D pCASL in preoperatively assessing the grade, cellular proliferation, and prognosis of gliomas. Additionally, we performed a subgroup analysis on patients with GBM.

MATERIALS AND METHODS

Patients

This was a retrospective study based on data collected from our prospective cohort of patients with gliomas who were hospitalized at the Department of Neurosurgery, Second Affiliated Hospital of Zhejiang University School of Medicine, between August 2013 and January 2015. This study was approved by the local ethics review board and was conducted in accordance with the ethical principles of the Declaration of Helsinki. Written informed consent was obtained from all participants. Fifty-eight patients with supratentorial cerebral gliomas, who underwent a preoperative MR imaging examination with a 3D pCASL sequence, were enrolled in this study. The preoperative Karnofsky Performance Scale (KPS) was administered in all patients when they were admitted to the hospital.

Imaging Data Acquisition

All subjects underwent MR imaging on a 3T system (Discovery MR750; GE Healthcare, Milwaukee, Wisconsin) with an 8-channel high-resolution receiver head coil. The CBF images were acquired with a 3D pCASL sequence with the following parameters: section thickness, 4 mm; number of sections, 36; FOV, 240 × 240 mm; matrix, 128 × 128; TR, 4632 ms; TE, 10.5 ms; flip angle, 111°; number of excitations, 3; labeling duration, 1450 ms; postlabeling duration, 1525 ms; and pixel bandwidth, 976.6 Hz/pixel. The scan time for this sequence was 4 minutes 29 seconds. In addition, a contrast-enhanced T2-FLAIR sequence was acquired after the injection of a gadolinium contrast agent.

Pathology

The median time interval between preoperative MR imaging and the operation was 4 days (range, 1–10 days). Three patients underwent only stereotactic biopsy, and the others underwent craniotomy. The histopathologic diagnosis was performed by pathologists on the basis of the WHO 2007 criteria.

The Ki-67 proliferating index was reported in 45 patients. In each case, areas with the highest number of positive-staining tumor nuclei were selected for calculating the Ki-67 index. According to previous literature,[23,24] patients with a Ki-67 index of ≥30% were assigned to the high Ki-67 index group and patients with a Ki-67 index of <30% were assigned to the low Ki-67 index group.

Follow-Up

Three patients who underwent stereotactic biopsy and 2 patients who died of operative complications were excluded in the postoperative follow-up. Among the other 53 patients, only 2 (3.9%) were lost to follow-up. Thus, 51 patients were included in the survival analysis. The median follow-up time was 30 months (range, 24–36 months). Overall survival (OS) was defined as the time from diagnosis until either death or the time the patient was last known to be alive (censused), and progression-free survival (PFS) was defined as the time from diagnosis until tumor progression, recurrence, or death or when the patient was last known to be alive (censused).[25]

Image Processing and Analysis

The CBF images were all coregistered to the contrast-enhanced T2-FLAIR images by using SPM12 (www.fil.ion.ucl.ac.uk/spm). The analysis of the images was performed with ImageJ, Version 1.49 (National Institutes of Health, Bethesda, Maryland). The ROIs were manually placed on the contrast-enhanced T2-FLAIR images by 1 expert neuroradiologist with 20 years' experience, who was blinded to the pathology of the tumors. Before ROIs were drawn, the image section that was speculated to contain the tumor area with the highest tumor blood flow was chosen by referring to the CBF maps. Areas with an abnormal signal in the enhanced T2-FLAIR images were all included. Another rectangular ROI was drawn to include contralateral gray matter areas. Then ROIs were copied to the corresponding CBF maps, as shown in Fig 1. The maximum CBF values (CBF_{max}) in ROIs were obtained. Then the relative CBF_{max} ($rCBF_{max}$) was calculated by dividing the CBF_{max} in the tumor ROI by the CBF_{max} in the contralateral ROI.

Interobserver Concordance

Another reader, a junior neurosurgeon who was blinded to the pathology, also delineated the ROIs of all tumors. The measurements from this reader were only used for the assessment of interobserver concordance. The $rCBF_{max}$ values measured by the 2 readers were compared by means of an intraclass correlation coefficient.

Statistical Analysis

All statistical analyses were performed with SPSS Statistics, Version 22 (IBM, Armonk, New York) and GraphPad Prism, Version 6.0 (GraphPad Software, San Diego, California). The significance level was set to $\alpha = .05$. $P < .05$ was statistically significant.

The normality assumption was tested with the Kolmogorov-Smirnov test. The data were expressed as mean ± SD. Interobserver reliability was with the intraclass correlation coefficient based on a 2-way random-effects model. The Pearson correlation analysis was used to assess the correlation among parameters.

The 1-way ANOVA followed by the Fisher least significant difference test was used to compare differences in parameters among multiple groups. The differences in parameters between the HGG and the LGG groups were compared using the independent samples *t* test. The receiver operating characteristic (ROC) curves for parameters in distinguishing HGG from LGG were generated. Optimal cutoff values were derived from ROC curves, and sensitivity, specificity, predictive values, and accuracy were calculated on the basis of these best cutoff values.

Survival analysis was conducted with the Cox regression for

both the univariate and multivariate analyses. Except for CBF parameters, 3 clinical features (age, sex, preoperative KPS) were also included in the survival analysis.

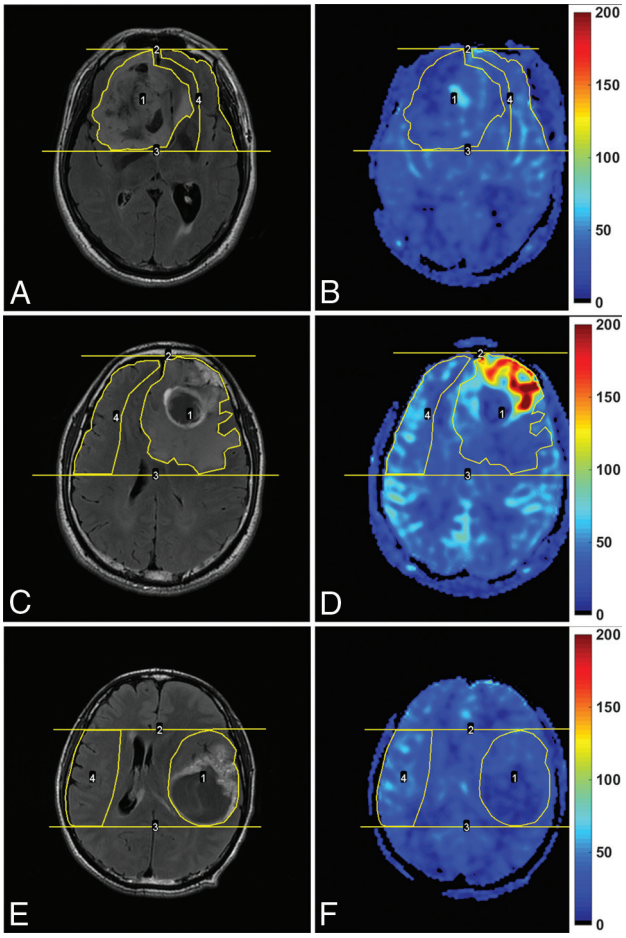

FIG 1. Enhanced T2-FLAIR images (*A*, *C*, and *E*) and CBF maps (*B*, *D*, and *F*) of a 69-year-old man with oligoastrocytoma (WHO grade II; Ki-67 index, 10%), a 42-year-old man with glioblastoma (WHO grade IV; Ki-67 index, 20%), and a 43-year-old man with glioblastoma (WHO grade IV; Ki-67 index, 60%), respectively. Note that blood flow is significantly elevated in the glioblastoma with a relatively low Ki-67 index, while it is not elevated in the glioblastoma with a very high Ki-67 index. The unit for CBF maps is milliliters/100 g/min.

RESULTS

Patient Characteristics

Among these 58 patients with gliomas, there were 27 women and 32 men, with a mean age of 49.5 years (range, 26–76 years) and a mean KPS score of 82.9 (range, 30–100). According to the WHO 2007 criteria, there were 13 patients diagnosed with WHO grade II (astrocytomas, $n = 5$; oligoastrocytomas, $n = 4$; oligodendrogliomas, $n = 4$), 17 patients diagnosed with WHO grade III (anaplastic astrocytomas, $n = 6$; anaplastic oligoastrocytomas, $n = 7$; anaplastic oligodendrogliomas, $n = 4$), and 28 patients diagnosed with WHO grade IV (GBM, $n = 28$).

Interobserver Concordance

The manifestations of an LGG, a GBM with a low Ki-67 index, and a GBM with a high Ki-67 index in contrast-enhanced T2-FLAIR images and CBF maps are shown in Fig 1. Our evaluation of the interobserver concordance for parameters showed excellent agreement. The intraclass correlation coefficients for the measurement of tumor CBF_{max}, contralateral CBF_{max}, and $rCBF_{max}$ were as high as 0.995, 0.860, and 0.987, respectively. Furthermore, there was a very strong correlation between CBF_{max} and $rCBF_{max}$ ($r = 0.941$).

Parameters in Each Type of Pathologic Tumor

The measured parameters in each type of pathologic tumor are summarized in Table 1. The CBF_{max} of GBMs was only significantly higher than that of astrocytomas ($P = .002$) and oligoastrocytomas ($P = .005$), while the $rCBF_{max}$ of GBMs was significantly higher than that of astrocytomas ($P < .001$), oligoastrocytomas ($P < .001$), oligodendrogliomas ($P = .032$), anaplastic astrocytomas ($P = .03$), and anaplastic oligoastrocytomas ($P = .027$). Both the CBF_{max} and $rCBF_{max}$ of GBMs were lower than those of anaplastic oligodendrogliomas without statistical significance (both $P = .22$).

Both the CBF_{max} and $rCBF_{max}$ of anaplastic oligodendrogliomas were significantly higher than those of anaplastic astrocytomas ($P = .035$ and .013, respectively) and anaplastic oligoastrocytomas ($P = .027$ and .012, respectively), while those of oligodendrogliomas were higher than those of astrocytomas ($P = .4$ and .35, respectively) and oligoastrocytomas ($P = .42$ and .30, respectively) without statistical significances. Both the CBF_{max} and $rCBF_{max}$ of anaplastic oligodendrogliomas were significantly higher than those of oligodendrogliomas ($P = .021$ and .012, respectively).

The mean CBF_{max} and $rCBF_{max}$ were similar between astrocytomas and oligoastrocytomas, or between anaplastic astrocytomas and anaplastic oligoastrocytomas. No significant differences were detected among different pathologic types for contralateral CBF_{max} ($P = .50$).

Parameters in Each Tumor Grade

Both the absolute tumor CBF_{max} and $rCBF_{max}$ increased with an increase in grade of glioma, as shown in Table 2. In all gliomas, both the CBF_{max} and $rCBF_{max}$ of grade IV gliomas were significantly

Table 1: Measurements of absolute CBF_{max} and $rCBF_{max}$ in each type of pathologic tumor

Grade/Histology	No.	CBF_{max} (mL/100 g/min)		$rCBF_{max}$
		Tumor	Contralateral	
Grade II ($n = 13$)				
Astrocytoma	5	75.4 ± 10.2[a,b]	83.2 ± 3.90	0.91 ± 0.18[c,d]
Oligoastrocytoma	4	74.8 ± 12.1[a,b]	93.2 ± 28.8	0.83 ± 0.16[c,d]
Oligodendroglioma	4	109.8 ± 47.8[e]	80.0 ± 9.6	1.38 ± 0.59[e,f]
Grade III ($n = 17$)				
Anaplastic astrocytoma	6	127.2 ± 84.8[e]	78.0 ± 23.6	1.51 ± 0.68[e,f]
Anaplastic oligoastrocytoma	7	125.1 ± 71.9[e]	82.4 ± 8.9	1.54 ± 0.88[e,f]
Anaplastic oligodendroglioma	4	212.5 ± 87.5	78.8 ± 16.6	2.75 ± 1.02
Grade IV ($n = 28$)				
Glioblastoma	28	171.5 ± 58.7	77.0 ± 10.9	2.25 ± 0.79

[a] $P < .01$, compared with glioblastoma.
[b] $P < .01$, compared with anaplastic oligoastrocytoma.
[c] $P < .001$, compared with glioblastoma.
[d] $P < .001$, compared with anaplastic oligoastrocytoma.
[e] $P < .05$, compared with anaplastic oligoastrocytoma.
[f] $P < .05$, compared with glioblastoma.

higher than those of grade II gliomas ($P < .001$), and those of grade III gliomas were significantly higher than those of grade II gliomas ($P = .011$ and .009, respectively), while those of grade IV gliomas were higher than those of grade III gliomas without statistical significance ($P = .198$ and .070, respectively). After oligodendrogliomas and anaplastic oligodendrogliomas were excluded, significant differences between grade III gliomas and grade IV gliomas were detected for both CBF_{max} and $rCBF_{max}$ ($P = .025$ and .004, respectively).

Differentiation of LGG and HGG

There were significant differences between LGG and HGG for both CBF_{max} and $rCBF_{max}$ ($P < .001$), regardless of whether oligodendrogliomas and anaplastic oligodendrogliomas were excluded, as shown in Fig 2. The ROC curves for CBF_{max} and $rCBF_{max}$ in distinguishing HGG from LGG are shown in Fig 3, and the results of the ROC analysis are shown in Table 3. The area under curve, best cutoff value, sensitivity, and specificity for CBF_{max} were 0.828, 91 (mL/100 g/min), 84.4%, and 84.6%, respectively, in all gliomas and were 0.859, 91 (mL/100 g/min), 82.9%, and 100%, respectively, after oligodendrogliomas and anaplastic oligodendrogliomas were excluded. Those for $rCBF_{max}$ were 0.863, 1.19, 82.2%, and 84.6%, respectively, in all gliomas and were 0.916, 1.22, 80.5%, and 100%, respectively, after oligodendrogliomas and anaplastic oligodendrogliomas were excluded. Both CBF_{max} and $rCBF_{max}$ values allowed HGGs to be distinguished from LGGs, and the differential diagnosis was improved after oligodendrogliomas and anaplastic oligodendrogliomas were excluded.

Table 2: Measurements of absolute CBF_{max} and $rCBF_{max}$ in each WHO grade with or without the exclusion of oligodendrogliomas and anaplastic oligodendrogliomas

Patients/Grades	No.	CBF_{max} (mL/100 g/min) Tumor	CBF_{max} (mL/100 g/min) Contralateral	$rCBF_{max}$
All				
Grade II	13	85.8 ± 30.3	85.3 ± 16.4	1.03 ± 0.41
Grade III	17	146.4 ± 84.0[b]	80.0 ± 16.1	1.81 ± 0.96[c]
Grade IV	28	171.5 ± 58.7[d]	77.0 ± 10.9	2.25 ± 0.15[d]
Excluded[a]				
Grade II	9	75.1 ± 10.4	87.7 ± 18.6	0.88 ± 0.16
Grade III	13	126.1 ± 74.7[e]	80.4 ± 16.6	1.52 ± 0.77[b]
Grade IV	28	171.5 ± 58.7[d,f]	77.0 ± 10.9	2.25 ± 0.15[d,g]

[a] With oligodendrogliomas and anaplastic oligodendrogliomas excluded. Note the following *P* values in each patient group:
[b] $P < .05$, compared with grade II.
[c] $P < .01$, compared with grade II.
[d] $P < .001$, compared with grade II.
[e] $P = .05$, compared with grade II.
[f] $P < .05$, compared with grade III.
[g] $P < .01$, compared with grade III.

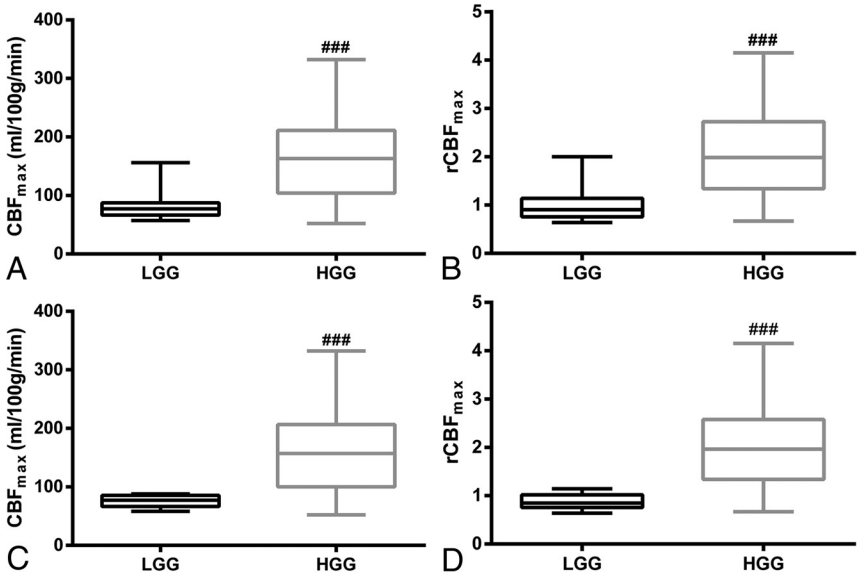

FIG 2. Boxplots of CBF_{max} (*A*) and $rCBF_{max}$ (*B*) in low-grade gliomas and high-grade gliomas for all subjects. The boxplots of CBF_{max} (*C*) and $rCBF_{max}$ (*D*) in LGGs and HGGs after the oligodendrogliomas and anaplastic oligodendrogliomas were excluded. ### indicates $P < .001$, compared with LGG.

Correlation with the Ki-67 Index

In all patients, as shown in Fig 4, both CBF_{max} ($P = .565$) and $rCBF_{max}$ ($P = .652$) values were not correlated with the Ki-67 index. However, there was a moderate positive association between CBF_{max} and the Ki-67 index in the low Ki-67 index group ($P = .029$, $r = 0.399$), and a high inverse association between CBF_{max} and the Ki-67 index in the high Ki-67 index group ($P < .001$, $r = -0.775$). Similarly, $rCBF_{max}$ had a moderate positive correlation with the Ki-67 index in the lower Ki-67 index group ($P = .017$, $r = 0.432$) and a high inverse correlation with the Ki-67 index in the high Ki-67 index group ($P < .001$, $r = -0.784$). In addition, in GBM, both CBF_{max} ($P = .017$, $r = -0.475$) and rCBFmax ($P = .006$, $r = -0.534$) showed a moderate negative correlation with the Ki-67 index.

Survival Analysis

Fifty-one patients (13 grade II, 13 grade III, 25 grade IV) were included in the survival analysis. Table 4 shows the results obtained with the univariate Cox model for PFS and OS in both gliomas and GBMs. Sex had no association with PFS or OS in both gliomas and GBMs (all data, $P > .5$). In gliomas, higher CBF_{max}, higher $rCBF_{max}$, older age, and lower KPS were associated with worse PFS (hazard ratio [HR] = 1.005, 1.670, 1.036, 0.971, respectively; all data, $P < .05$), while CBF_{max} and $rCBF_{max}$ were not prognosis factors for OS ($P = .244$ and .232, respectively). In GBMs, lower CBF_{max}, lower $rCBF_{max}$, and older age tended to be associated with worse OS without statistical significances (HR = 0.993, 0.563, 1.030, respectively; $P = .070$, .065, and .103, respectively), while CBF_{max} and $rCBF_{max}$ were not associated with PFS ($P = .497$ and .644, respectively).

Either CBF_{max} or $rCBF_{max}$ were included in the multivariate Cox analysis for PFS in gliomas, together with age and KPS. Furthermore, CBF_{max} or $rCBF_{max}$ were also included in the multivariate Cox analysis for OS in GBM, together with age. The results showed that $rCBF_{max}$ was a significant independent prognostic factor for PFS in gliomas

($P = .005$) and OS in GBMs ($P = .033$), while CBF_{max} was only a significant independent prognosis factor for PFS in gliomas ($P = .008$), shown in Table 5. After adjustment for age, higher CBF_{max} (HR = 1.007) and higher $rCBF_{max}$ (HR = 1.707) were associated with worse PFS in gliomas, while higher $rCBF_{max}$ (HR = 0.490) was associated with better OS in GBM.

DISCUSSION

In this study, 3D pCASL-derived CBF maps were found to be effective in preoperatively assessing the grade and prognosis in gliomas. Another interesting finding was that CBF_{max} and $rCBF_{max}$ showed a dual relationship with the degree of malignancy in gliomas. In accordance with previous studies based on pulsed ASL and CASL,[8-17] both CBF_{max} and $rCBF_{max}$ obtained from pCASL increased with increasing grade of gliomas, and gliomas with higher CBF_{max} and $rCBF_{max}$ were associated with worse PFS. These findings suggest that gliomas with higher $rCBF_{max}$ are associated with a higher degree of malignancy. However, in GBMs, both CBF_{max} and $rCBF_{max}$ were found to have a significant negative correlation with the Ki-67 index. Also, GBMs with a lower $rCBF_{max}$ were associated with worse OS after adjustment for age. Thus, GBMs with lower blood flow seemed to be more aggressive.

Unlike quantification methods of DSC MR imaging, which require an accurate arterial input function, 1 advantage of the ASL sequence is that it can provide an absolute quantification of CBF.[9] In our study, a very strong correlation between CBF_{max} and $rCBF_{max}$ was reported. The results of $rCBF_{max}$ were similar to those of CBF_{max} in grading gliomas and evaluating the Ki-67 index, while $rCBF_{max}$ seemed to be more valuable in predicting the prognosis of gliomas and GBMs. These results suggest that ASL-derived absolute CBF is also useful in evaluating gliomas.

However, compared with the DSC perfusion MR imaging, one limitation of the application of ASL is the relatively low SNR.[15,20]

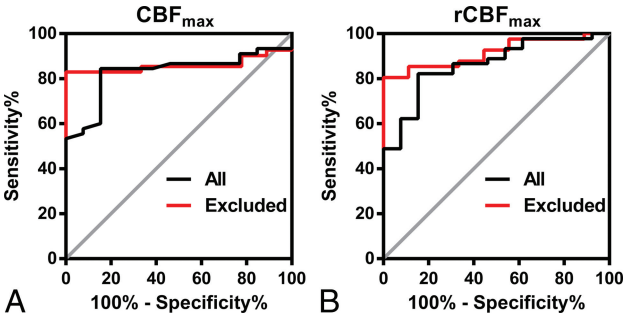

FIG 3. Receiver operating characteristic curves of CBF_{max} (*A*) and $rCBF_{max}$ (*B*) in distinguishing high- from low-grade gliomas, without (*black line*) or with (*red line*) oligodendrogliomas and anaplastic oligodendrogliomas excluded.

Table 3: ROC curve analyses of CBF_{max} and $rCBF_{max}$ in discriminating high- and low-grade gliomas

Parameters/Patients	AUC	Youden Index	Cutoff Value	Sensitivity (%)	Specificity (%)	PPV (%)	NPV (%)	Accuracy (%)
CBF_{max}								
All	0.828	0.690	91 mL/100 g/min	84.4	84.6	95.0	61.1	84.5
Excluded[a]	0.859	0.829	91 mL/100 g/min	82.9	100	100	56.3	86.0
$rCBF_{max}$								
All	0.863	0.668	1.19	82.2	84.6	94.9	57.9	82.8
Excluded[a]	0.916	0.805	1.22	80.5	100	100	52.9	84.0

Note:—AUC indicates area under the curve; PPV, positive predictive value; NPV, negative predictive value.
[a] With oligodendrogliomas and anaplastic oligodendrogliomas excluded.

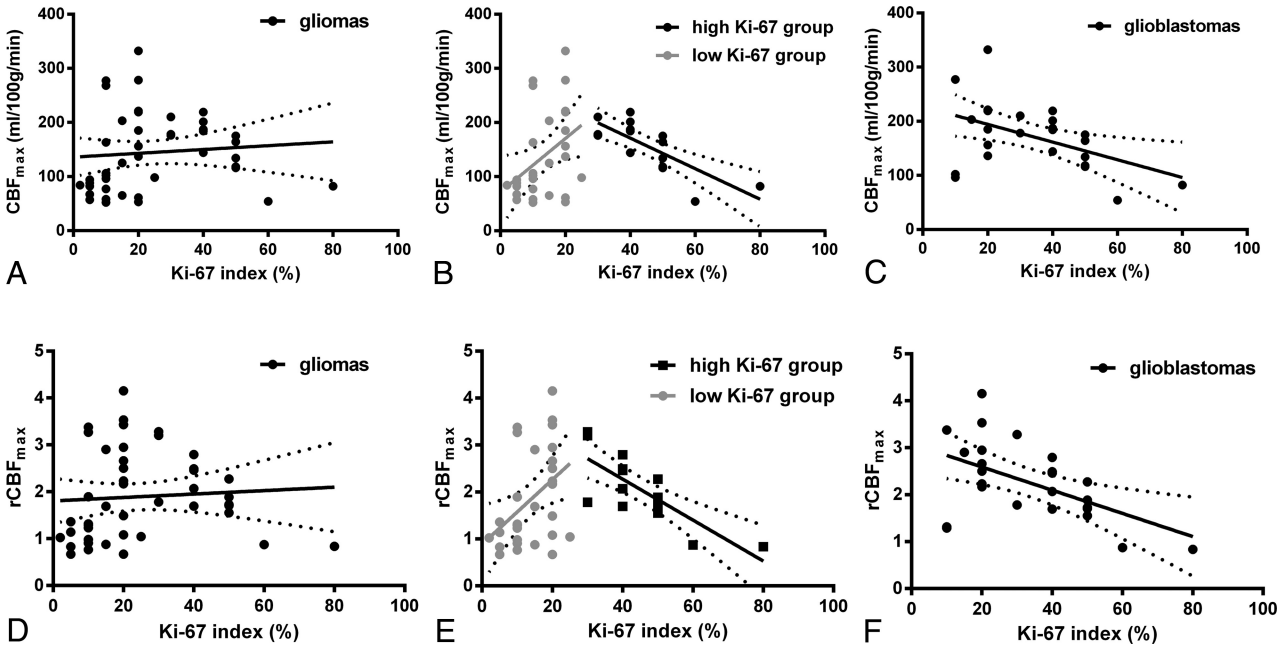

FIG 4. The linear regression of CBF_{max} (*A–C*) and $rCBF_{max}$ (*D–F*) with the Ki-67 index in all subjects (*A* and *D*), in the low and high Ki-67 groups (*B* and *E*), and in glioblastomas (*C* and *F*). The low Ki-67 group included patients with a Ki-67 index of <30%, and the high Ki-67 group included patients with a Ki-67 index of ≥30%.

CASL is an improved method, providing a higher tagging efficiency compared with pulsed ASL.[18] However, because of magnetization transfer effects, the magnetization in the target tissues will be reduced, which limits the application of this method.[18] In 2005, Garcia el al[19] proposed the pCASL method to overcome this disadvantage, and this method can improve not only the SNR but also the accuracy of CBF measurements.[18,20] Previous studies have shown that the pulsed ASL–derived and CASL-derived CBF maps have potential value in grading gliomas.[8,10-15] In the current study, pCASL-derived CBF maps were also found to be effective in grading gliomas. However, a previous study indicated that pCASL-derived CBF maps were unable to grade gliomas, in contradiction to our results.[21] In that study, compared with relative CBF derived from the dynamic contrast-enhanced MR imaging, the ASL-derived relative CBF was found to be relatively higher in LGGs but lower in HGGs. The potential explanation is not clear. More research may be required to evaluate the reliability of the CBF maps derived from pCASL.

Oligodendrogliomas and anaplastic oligodendrogliomas exhibit elevated relative CBV compared with astrocytic tumors of the same histologic grade.[26,27] Similarly, our study also found that both CBF_{max} and $rCBF_{max}$ were clearly elevated in oligodendrogliomas (not statistically significant) and anaplastic oligodendrogliomas (statistically significant) compared with other pathologic subtypes of the same histologic grade. In accordance with previous studies based on relative CBV,[26] ability of the CBF_{max} and $rCBF_{max}$ values in differentiating HGGs from LGGs improved after we excluded oligodendrogliomas and anaplastic oligodendrogliomas.

Furthermore, our results demonstrated a significantly higher CBF_{max} and $rCBF_{max}$ in anaplastic oligodendrogliomas than in oligodendrogliomas. These results conflicted with those of a previous study based on CASL-derived CBF_{max}.[12] However, a recent study by Fellah et al,[28] based on DSC-derived relative CBF, reported a result similar to that in our study. Several previous studies have also shown a significantly higher relative CBV in anaplastic oligodendrogliomas than in oligodendrogliomas,[28-31] while some other studies have reported a conflicting result.[32-34] The ability of perfusion parameters to distinguish oligodendrogliomas and anaplastic oligodendrogliomas needs to be evaluated further.

A previous study by Mayer et al[22] showed a positive correlation between proliferative activity and the level of a hypoxia biomarker in GBM. This molecular pathology finding is consistent with our finding that the Ki-67 index had a negative correlation with CBF_{max} and $rCBF_{max}$ in GBMs. However, the potential mechanism is not clear. Evans et al[35] found that higher grade gliomas were associated with more hypoxia. It is widely accepted that hypoxia will lead to the activation of the transcription of hypoxia-inducible factor-1 via stabilization of its α subunit.[36-38] One potential mechanism of this may result in lower tumor blood flow in GBMs, which causes severe hypoxia and, in turn, the activation of the transcription of hypoxia-inducible factor-1, leading to high proliferative activity through further downstream pathways. Another potential mechanism might be due to the inability of angiogenesis to keep up with tumor cell proliferation in certain GBMs that have a high proliferative activity. The explicit mechanism needs to be investigated further.

On the other hand, our study also found that GBMs with a lower $rCBF_{max}$ were associated with a worse OS but showed no association with PFS. This finding also suggests that a GBM with lower blood flow may cause severe hypoxia, causing it to become increasingly malignant. Some other studies have also found that hypoxia in GBM is related to a poor prognosis,[39] yet 2 previous studies based on ASL-derived CBF maps have reported a contradictory result.[16,17] However, 1 of those contradictory studies involved only 18 gliomas,[16] and another contradictory study had only performed qualitative analysis,[17] which reduced their reliability. It is well-known that the activity of hypoxia-inducible factor-1α–mediated pathways due to hypoxia will lead to migration and invasion of tumor cells.[40,41] In addi-

Table 4: Univariate Cox model for progression-free survival and overall survival in patients with gliomas and glioblastomas

	PFS			OS		
Variables	HR	95% CI	*P* Value	HR	95% CI	*P* Value
Gliomas ($n = 51$)						
Age	1.036	1.009–1.063	.008	1.043	1.014–1.073	.004
Sex[a]	0.957	0.670–1.368	.811	0.896	0.606–1.325	.582
KPS	0.971	0.953–0.989	.002	0.970	0.952–0.988	.002
CBF_{max}	1.005	1.001–1.010	.027	1.003	0.998–1.008	.244
$rCBF_{max}$	1.670	1.149–2.427	.007	1.246	0.869–1.785	.232
GBM ($n = 25$)						
Age	1.036	1.002–1.072	.039	1.030	0.994–1.067	.103
Sex[a]	0.851	0.547–1.323	.851	0.870	0.548–1.381	.555
KPS	0.986	0.963–1.008	.215	0.987	0.965–1.009	.242
CBF_{max}	0.997	0.989–1.005	.497	0.993	0.985–1.001	.070
$rCBF_{max}$	0.865	0.467–1.601	.644	0.563	0.306–1.035	.065

[a] Female versus male.

Table 5: Multivariate Cox model for progression-free survival in patients with gliomas and overall survival in patients with glioblastomas

		PFS in Gliomas			OS in GBM		
Parameters	Variables	HR	95% CI	*P* Value	HR	95% CI	*P* Value
Multivariate Cox model including CBF_{max}	CBF_{max}	1.007	1.002–1.012	.008	0.992	0.984–1.001	.066
	Age	1.043	1.015–1.071	.002	1.030	0.995–1.067	.097
	KPS[a]	–	–	.131[b]	–	–	–
Multivariate Cox model including $rCBF_{max}$	$rCBF_{max}$	1.707	1.174–2.483	.005	0.490	0.254–0.943	.033
	Age	1.038	1.011–1.065	.006	1.037	1.001–1.074	.045
	KPS[a]	–	–	.233[b]	–	–	–

[a] KPS was not included in the multivariate Cox analysis for OS in glioblastomas.

[b] Only the *P* value was presented for the variable, which was excluded from the Cox model with $P > .10$.

tion, hypoxia is known to induce resistance to radiation therapy and chemotherapy through several mechanisms.[42,43] This could explain why GBMs with a lower blood flow were more aggressive and were associated with a worse OS.

However, a previous study by Law et al[44] in 2008 found that GBMs with high relative CBV were significantly associated with a poor OS, while another study by Deike et al[45] in 2016 suggested that GBMs with a low blood supply may be associated with poor OS. The difference in results between these studies may be due to the different postoperative treatment strategies. Currently, concomitant radiochemotherapy has become the standard treatment for GBMs, and sometimes bevacizumab is also used to treat recurrent GBMs. Thus, resistance to radiation therapy and chemotherapy is now playing a more important role than before in the treatment of GBMs and will clearly influence the OS of patients with GBMs. A prospective study enrolling relatively large samples is needed to accurately evaluate the role of perfusion parameters in predicting the outcome of GBMs.

There were some limitations in our research. First, the sample size used for this study was not very large; therefore, some of the results may not be completely reliable, especially the results from the subgroup analysis. Further studies enrolling larger samples are needed to verify these results. Second, the postcontrast T2-FLAIR images were consulted when drawing the ROIs, so the ROI selection method presented in our study was not an accurate portrayal of a blind study. However, the resulting bias is hardly avoided, and it has also existed in many previous studies.[8-14] Compared with previous ROI selection methods, the method presented in our study is relatively objective, with an excellent intraclass correlation coefficient. Third, molecular pathology for gliomas, such as 1p19q deletion and *IDH1/2* mutations, was not routinely examined in our study. Further studies dividing gliomas or GBMs into subgroups by molecular pathology may provide further useful information.

CONCLUSIONS

3D pCASL-derived CBF maps are effective in preoperative evaluation of gliomas. Although gliomas with higher blood flow are associated with a higher degree of malignancy, GBMs with a lower blood flow are likely to be more aggressive.

ACKNOWLEDGMENTS

We thank Professor Yi Shen from the Department of Public Health, Zhejiang University School of Medicine, for his assistance in statistics, and Harry Lee from Zhejiang University for his assistance in editing the manuscript.

Disclosures: Qiang Zeng—*RELATED*: *Grant*: Hangzhou Municipal Health Bureau; *UNRELATED*: *Employment*: Second Affiliated Hospital of Zhejiang University College of Medicine. Biao Jiang—*RELATED*: *Grant*: Zhejiang Provincial Natural Science Foundation Committee; *UNRELATED*: *Employment*: Second Affiliated Hospital of Zhejiang University College of Medicine. Chenhan Ling—*RELATED*: *Grant*: Hangzhou Municipal Health Bureau; *UNRELATED*: *Employment*: Second Affiliated Hospital of Zhejiang University College of Medicine. Fei Dong—*UNRELATED*: *Employment*: Second Affiliated Hospital of Zhejiang University College of Medicine. Jianmin Zhang—*UNRELATED*: *Employment*: Second Affiliated Hospital of Zhejiang University College of Medicine; *Grants/Grants Pending*: The National Natural Science Foundation of China.

REFERENCES

1. Schwartzbaum JA, Fisher JL, Aldape KD, et al. **Epidemiology and molecular pathology of glioma.** *Nat Clin Pract Neurol* 2006;2:494–503 CrossRef Medline
2. Weller M, van den Bent M, Hopkins K, et al; European Association for Neuro-Oncology (EANO) Task Force on Malignant Glioma. **EANO guideline for the diagnosis and treatment of anaplastic gliomas and glioblastoma.** *Lancet Oncol* 2014;15:e395–e403 CrossRef Medline
3. Soffietti R, Baumert BG, Bello L, et al; European Federation of Neurological Societies. **Guidelines on the management of low-grade gliomas: report of an EFNS-EANO Task Force.** *Eur J Neurol* 2010;17:1124–33 CrossRef Medline
4. Roy B, Gupta RK, Maudsley AA, et al. **Utility of multiparametric 3-T MRI for glioma characterization.** *Neuroradiology* 2013;55:603–13 CrossRef Medline
5. Nguyen TB, Cron GO, Perdrizet K, et al. **Comparison of the diagnostic accuracy of DSC- and dynamic contrast-enhanced MRI in the preoperative grading of astrocytomas.** *AJNR Am J Neuroradiol* 2015;36:2017–22 CrossRef Medline
6. Knopp EA, Cha S, Johnson G, et al. **Glial neoplasms: dynamic contrast-enhanced T2*-weighted MR imaging.** *Radiology* 1999;211:791–98 CrossRef Medline
7. Law M, Yang S, Babb JS, et al. **Comparison of cerebral blood volume and vascular permeability from dynamic susceptibility contrast-enhanced perfusion MR imaging with glioma grade.** *AJNR Am J Neuroradiol* 2004;25:746–55 Medline
8. Furtner J, Schöpf V, Schewzow K, et al. **Arterial spin-labeling assessment of normalized vascular intratumoral signal intensity as a predictor of histologic grade of astrocytic neoplasms.** *AJNR Am J Neuroradiol* 2014;35:482–89 CrossRef Medline
9. Rau MK, Braun C, Skardelly M, et al. **Prognostic value of blood flow estimated by arterial spin labeling and dynamic susceptibility contrast-enhanced MR imaging in high-grade gliomas.** *J Neurooncol* 2014;120:557–66 CrossRef Medline
10. Fudaba H, Shimomura T, Abe T, et al. **Comparison of multiple parameters obtained on 3T pulsed arterial spin-labeling, diffusion tensor imaging, and MRS and the Ki-67 labeling index in evaluating glioma grading.** *AJNR Am J Neuroradiol* 2014;35:2091–98 CrossRef Medline
11. Kim HS, Kim SY. **A prospective study on the added value of pulsed arterial spin-labeling and apparent diffusion coefficients in the grading of gliomas.** *AJNR Am J Neuroradiol* 2007;28:1693–99 CrossRef Medline
12. Chawla S, Wang S, Wolf RL, et al. **Arterial spin-labeling and MR spectroscopy in the differentiation of gliomas.** *AJNR Am J Neuroradiol* 2007;28:1683–89 CrossRef Medline
13. Warmuth C, Gunther M, Zimmer C. **Quantification of blood flow in brain tumors: comparison of arterial spin labeling and dynamic susceptibility-weighted contrast-enhanced MR imaging.** *Radiology* 2003;228:523–32 CrossRef Medline
14. Kim MJ, Kim HS, Kim JH, et al. **Diagnostic accuracy and interobserver variability of pulsed arterial spin labeling for glioma grading.** *Acta Radiol* 2008;49:450–57 CrossRef Medline
15. Wolf RL, Wang J, Wang S, et al. **Grading of CNS neoplasms using continuous arterial spin labeled perfusion MR imaging at 3 Tesla.** *J Magn Reson Imaging* 2005;22:475–82 CrossRef Medline
16. Furtner J, Bender B, Braun C, et al. **Prognostic value of blood flow measurements using arterial spin labeling in gliomas.** *PLoS One* 2014;9:e99616 CrossRef Medline
17. Qiao XJ, Ellingson BM, Kim HJ, et al. **Arterial spin-labeling perfusion MRI stratifies progression-free survival and correlates with epidermal growth factor receptor status in glioblastoma.** *AJNR Am J Neuroradiol* 2015;36:672–77 CrossRef Medline
18. Wong EC. **New developments in arterial spin labeling pulse sequences.** *NMR Biomed* 2013;26:887–91 CrossRef Medline
19. Garcia DM, De Bazelaire C, Alsop D. **Pseudo-continuous flow driven adiabatic inversion for arterial spin labeling.** *Proc Int Soc Magn Reson Med* 2005;13:37

20. Fernández-Seara MA, Edlow BL, Hoang A, et al. **Minimizing acquisition time of arterial spin labeling at 3T.** *Magn Reson Med* 2008;59:1467–71 CrossRef Medline
21. Roy B, Awasthi R, Bindal A, et al. **Comparative evaluation of 3-dimensional pseudocontinuous arterial spin labeling with dynamic contrast-enhanced perfusion magnetic resonance imaging in grading of human glioma.** *J Comput Assist Tomogr* 2013;37:321–26 CrossRef Medline
22. Mayer A, Schneider F, Vaupel P, et al. **Differential expression of HIF-1 in glioblastoma multiforme and anaplastic astrocytoma.** *Int J Oncol* 2012;41:1260–70 CrossRef Medline
23. Schaffel R, Hedvat CV, Teruya-Feldstein J, et al. **Prognostic impact of proliferative index determined by quantitative image analysis and the International Prognostic Index in patients with mantle cell lymphoma.** *Ann Oncol* 2010;21:133–39 CrossRef Medline
24. Bottini A, Berruti A, Brizzi MP, et al. **Cytotoxic and antiproliferative activity of the single agent epirubicin versus epirubicin plus tamoxifen as primary chemotherapy in human breast cancer: a single-institution phase III trial.** *Endocr Relat Cancer* 2005;12:383–92 CrossRef Medline
25. Jain R, Poisson LM, Gutman D, et al. **Outcome prediction in patients with glioblastoma by using imaging, clinical, and genomic biomarkers: focus on the nonenhancing component of the tumor.** *Radiology* 2014;272:484–93 CrossRef Medline
26. Lev MH, Ozsunar Y, Henson JW, et al. **Glial tumor grading and outcome prediction using dynamic spin-echo MR susceptibility mapping compared with conventional contrast-enhanced MR: confounding effect of elevated rCBV of oligodendroglimoas [corrected].** *AJNR Am J Neuroradiol* 2004;25:214–21 Medline
27. Cha S, Tihan T, Crawford F, et al. **Differentiation of low-grade oligodendrogliomas from low-grade astrocytomas by using quantitative blood-volume measurements derived from dynamic susceptibility contrast-enhanced MR imaging.** *AJNR Am J Neuroradiol* 2005;26:266–73 Medline
28. Fellah S, Caudal D, De Paula AM, et al. **Multimodal MR imaging (diffusion, perfusion, and spectroscopy): is it possible to distinguish oligodendroglial tumor grade and 1p/19q codeletion in the pretherapeutic diagnosis?** *AJNR Am J Neuroradiol* 2013;34:1326–33 CrossRef Medline
29. Kapoor GS, Gocke TA, Chawla S, et al. **Magnetic resonance perfusion-weighted imaging defines angiogenic subtypes of oligodendroglioma according to 1p19q and EGFR status.** *J Neurooncol* 2009;92:373–86 CrossRef Medline
30. Whitmore RG, Krejza J, Kapoor GS, et al. **Prediction of oligodendroglial tumor subtype and grade using perfusion weighted magnetic resonance imaging.** *J Neurosurg* 2007;107:600–09 CrossRef Medline
31. Spampinato MV, Smith JK, Kwock L, et al. **Cerebral blood volume measurements and proton MR spectroscopy in grading of oligodendroglial tumors.** *AJR Am J Roentgenol* 2007;188:204–12 CrossRef Medline
32. Jenkinson MD, Smith TS, Joyce KA, et al. **Cerebral blood volume, genotype and chemosensitivity in oligodendroglial tumours.** *Neuroradiology* 2006;48:703–13 CrossRef Medline
33. Hilario A, Ramos A, Perez-Nuñez A, et al. **The added value of apparent diffusion coefficient to cerebral blood volume in the preoperative grading of diffuse gliomas.** *AJNR Am J Neuroradiol* 2012;33:701–07 CrossRef Medline
34. Xu M, See SJ, Ng WH, et al. **Comparison of magnetic resonance spectroscopy and perfusion-weighted imaging in presurgical grading of oligodendroglial tumors.** *Neurosurgery* 2005;56:919–26 CrossRef Medline
35. Evans SM, Judy KD, Dunphy I, et al. **Hypoxia is important in the biology and aggression of human glial brain tumors.** *Clin Cancer Res* 2004;10:8177–84 CrossRef Medline
36. Korkolopoulou P, Patsouris E, Konstantinidou AE, et al. **Hypoxia-inducible factor 1alpha/vascular endothelial growth factor axis in astrocytomas: associations with microvessel morphometry, proliferation and prognosis.** *Neuropathol Appl Neurobiol* 2004;30:267–78 CrossRef Medline
37. Mashiko R, Takano S, Ishikawa E, et al. **Hypoxia-inducible factor 1alpha expression is a prognostic biomarker in patients with astrocytic tumors associated with necrosis on MR image.** *J Neurooncol* 2011;102:43–50 CrossRef Medline
38. Birner P, Piribauer M, Fischer I, et al. **Vascular patterns in glioblastoma influence clinical outcome and associate with variable expression of angiogenic proteins: evidence for distinct angiogenic subtypes.** *Brain Pathol* 2003;13:133–43 Medline
39. Bekaert L, Valable S, Lechapt-Zalcman E, et al. **[18F]-FMISO PET study of hypoxia in gliomas before surgery: correlation with molecular markers of hypoxia and angiogenesis.** *Eur J Nucl Med Mol Imaging* 2017;44:1383–92 CrossRef Medline
40. Fujiwara S, Nakagawa K, Harada H, et al. **Silencing hypoxia-inducible factor-1alpha inhibits cell migration and invasion under hypoxic environment in malignant gliomas.** *Int J Oncol* 2007;30:793–802 Medline
41. Zagzag D, Lukyanov Y, Lan L, et al. **Hypoxia-inducible factor 1 and VEGF upregulate CXCR4 in glioblastoma: implications for angiogenesis and glioma cell invasion.** *Lab Invest* 2006;86:1221–32 CrossRef Medline
42. Toth RK, Warfel NA. **Strange bedfellows: nuclear factor, erythroid 2-like 2 (Nrf2) and hypoxia-inducible factor 1 (HIF-1) in tumor hypoxia.** *Antioxidants* 2017;6:27 CrossRef Medline
43. Liu H, Cai Y, Zhang Y, et al. **Development of a hypoxic radiosensitizer-prodrug liposome delivery DNA repair inhibitor Dbait combination with radiotherapy for glioma therapy.** *Adv Healthc Mater* 2017;6:1601377 CrossRef Medline
44. Law M, Young RJ, Babb JS, et al. **Gliomas: predicting time to progression or survival with cerebral blood volume measurements at dynamic susceptibility-weighted contrast-enhanced perfusion MR imaging.** *Radiology* 2008;247:490–98 CrossRef Medline
45. Deike K, Wiestler B, Graf M, et al. **Prognostic value of combined visualization of MR diffusion and perfusion maps in glioblastoma.** *J Neurooncol* 2016;126:463–72 CrossRef Medline